Journal of the American Association for Laboratory Animal Science
Copyright 2025
by the American Association for Laboratory Animal Science

Vol 64, No 3
May 2025
Pages 356–363

Defining Normative Mixed-Breed Ovine Spine Anatomy Using Computed Tomography and Magnetic Resonance Imaging

Yazan Shamli Oghli, MS,[1] Nicki Mara Barka, BS,[2] Tina Billstrom, MS,[2] David Dinsmoor, MS,[2] and Kevin Hines, MD[1,*]

The availability of suitable preclinical models is critical for developing novel therapeutic interventions. Ovine models are particularly useful for studying spinal diseases due to their similarity in size and weight to humans. However, evaluation of the ovine spinal cord and canal anatomy is necessary for such translational application. To date, no studies have quantified the entire ovine spine using advanced imaging. In this work, we used MR and CT imaging to obtain the quantitative anatomic information necessary for the appropriate preclinical investigations of the spinal cord and spine using sheep. Six mixed-breed, female sheep were scanned in dorsal recumbency for MR T1- and T2-weighted images, as well as sternal and dorsal recumbency for CT images. Interactive multiplanar reformation and a series of automatic measurements, followed by computation of various distances within the spinal cord and canal, were completed for each animal. This led to the quantification of the MR-derived images: spinal cord and canal width and height, cord circumference, dorsal CSF distance, and ventral-dorsal/left-right vertebral displacements. The CT-derived, computed measurements were for aminal circumference, vertebral height, and disk height index. CT and MR imaging were performed on all animals, although some measurements were excluded due to image quality. Spinal cord circumference peaked at C6 (27.41 mm) and L6 (24.93 mm), with notable ventral-dorsal displacement at L7 (2.65 mm). Neural foramina circumference showed bimodal peaks at C8 and L7, while vertebral height declined from L7 to T9, peaking at C4 (40.42 mm), highlighting structural variability along the spine. This study will be beneficial in the modeling and development of precision neurosurgical treatments by providing a comprehensive quantitative dataset for veterinary research on spinal disease and the development of therapeutic interventions.

Abbreviations and Acronyms: CSF, cerebrospinal fluid; DHI, disk height index; MPR, multiplanar reformation; SCS, spinal cord stimulation; SCI, spinal cord injury; TSE, turbo spin echo

DOI: 10.30802/AALAS-JAALAS-24-148

Introduction

Animal models are used to assess underlying mechanisms of action and test the safety, efficacy, and feasibility of interventional spinal and neuromodulation therapies before clinical translation. Ovine models of neurologic conditions, particularly of the spine, are valuable due to the similarity in size and anatomic features of the sheep spine as compared with humans.[1] One such model, the use of spinal cord stimulation (SCS) for pain, remains incomplete.[2,3] Evoked compound action potential (ECAP) sensing in sheep has been used to gain foundational mechanistic insight into SCS waveforms that would otherwise be difficult to obtain in rodents or humans.[4] Furthermore, ovine can be trained for biomechanical and gait tests, and their brain recordings have been used to study the effects of SCS in neuropathic pain.[5–8] Ovine models of spinal cord injury (SCI) have also been investigated, including the effects of SCS on gait improvement.[9,10] Other models that have been investigated include percutaneous spinal ablations as well as compressive myelopathy ovine models.[11,12] However, studies lack normative evaluation of the ovine spine anatomy, which limits the generalizability of research involving the implantation of devices intended for human use and for further study of ovine spine morphology.

A recent study established comparative, high-resolution MRI lumbosacral spine atlases of several species using cadaveric specimens, particularly of the rat, cat, pig, monkey, and human.[13] The authors investigated the length of spinal cord segments, vertebral enlargements, morphologic characteristics, as well as gray and white matter cross-sectional lengths and widths. In current literature, such radiographic measurements have only been documented in the ovine lumbar spine. The current body of literature also lacks studies combining CT and MRI evaluation of the ovine spine.[1,14,15] Further characterization of the ovine spine, including cervical and thoracic studies, would help inform the clinical translation of potential interventional pain procedures and serve as a guide to better understand treatment mechanisms and predict treatment response.

To this end, the purpose of the present study was to conduct a normative quantitative characterization of the ovine spine and its components using MRI and CT. We imaged the complete spine and conducted measurements to characterize the spinal canal, neural foramen, disk height, spinal cord, CSF, and vertebrae in sheep. Eventually, such measures may be important to continued advancements in the development of interventional pain procedures, such as precision closed-loop

Submitted: 02 Dec 2024. Revision requested: 06 Jan 2025. Accepted: 17 Mar 2025.
[1]Department of Neurosurgery, Thomas Jefferson University, Philadelphia, Pennsylvania; and [2]Medtronic plc, Minneapolis, Minnesota
**Corresponding author. Email: kevin.hines@jefferson.edu*
This article contains supplemental materials online.

SCS in ovine models, as well as elucidating the mechanistic underpinnings of neurologic diseases by leveraging the ovine preclinical model.

Methods

Subjects. This study was approved by the Medtronic IACUC before completing any work. The animals were cared for according to the USDA Animal Welfare Act standards, Medtronic Physiologic Research Laboratories Standard Operating Procedures, and the *Guide for the Care and Use of Laboratory Animals* (8th ed). Female sheep (n = 6; 8 to 19 mo old; 52 to 75.5 kg) of mixed breeds (mixed Polypay [n = 3], Friesian [n = 2], and mixed Friesian [n = 1]) were used; females were used to avoid complications with urolithiasis, a common disease of male sheep. In addition, the temperament of ewes is better suited to their use in a controlled laboratory environment compared with that of rams. The animals were sourced from Central Minnesota Livestock Sourcing. The animals were housed in a colony in a temperature and humidity-controlled environment with a 12 ± 1-h light/dark cycle. Water was supplied ad libitum, and the ovine were fed free choice hay for 4 to 8 h/day, along with a standard 3 cups/day of commercial sheep pelleted diet.

Anesthesia and imaging. Each animal was premedicated with 400 µg (5.3 to 7.7 µg/kg) of fentanyl and anesthesia was induced with propofol (250 to 400 mg, 5.3 to 6.7 mg/kg); anesthesia was then maintained using isoflurane (1.8% to 3.1%). The fentanyl and propofol were delivered intravenously via the saphenous vein. Full-spine MR (1.5T Ingenia; Philips Healthcare) and CT (SOMATOM Dual Source; Siemens) imaging was then performed on each animal. The animals were euthanized after the study data collection. For the MR imaging, the animals were first placed in dorsal recumbency and secured to the table to reduce motion artifact. A radiolucent, vinyl positioning strap with hook-and-loop closure around the table and torso of the animals was used for this purpose. This position is consistent with how imaging is performed in humans preoperatively. The cervical, thoracic, and lumbar spine were imaged separately, but special care was given to ensure overlap between sections to allow for counting of the vertebrae. The following sequences were then employed:

(1) T2-weighted TSE (turbo spin echo) sagittal: This sequence utilized an approximate 450-mm^2 field-of-view (FOV) depending on the coverage area, approximately 13 to 15 slices to cover the vertebral bodies edge-to-edge and a slice thickness of 2 to 3 mm.
(2) T2-weighted TSE transverse, angled with the vertebral bodies: This sequence utilized a 320-mm^2 FOV, approximately 60 slices to cover the vertebral bodies in each section, and a slice thickness of 3 to 6 mm depending on the coverage area.
(3) T1 3-dimensional (3D) transverse: This sequence utilized a 250-mm^2 FOV, 360 slices, and a slice thickness of 2 mm.

CT images were acquired in both sternal and dorsal recumbency. For the sternal recumbency imaging, the haunches were supported to keep the spine both in a horizontal plane and as straight as possible for image collection. For the dorsal recumbency imaging, the legs were secured to allow the spine to be as close to the isocenter as possible without gantry interference. For both the prone and supine sequences, the entire spine (cervical to tail) was imaged in a single pass using a 3 × 0.5-mm B50 kernel. The prone images were selected for use in this work; with the animal supine on the concave table.

Analysis and image processing. A comprehensive series of manual assessments and automated morphometrics was performed using the images acquired from each ovine. The images were prepared by first importing from Digital Imaging and Communications in Medicine (DICOM) format into Materialise Interactive Medical Image Control System (MIMICS; v24.0; Materialise). The images were then segregated by imaging sequence type, with all postprocessing completed within MIMICS. Next, interactive multiplanar reformation (MPR) was used to tailor each vertebral segment view. Initial assessments included the number of vertebrae in each spinal segment and the location of the conus medullaris using the sagittal T2 TSE scans.

Two sets of automated measurements were then collected. For the first set, a multistep process was followed that included using the MPR function with the transverse T2 sequences to draw splines, planes, and point-to-point lines around both the spinal cord and canal dura at the midvertebral body for each segment. Special care was taken to ensure that the splines were drawn in the transverse plane, which was most orthogonal to the spinal column to avoid exaggeration of measurements due to foreshortening/elongation. A coronal plane was fit at the widest point of the spline encompassing the spinal cord at every level of the spine individually due to the curvature. A second sagittal plane, orthogonal to the coronal plane, was then applied. A Python (v3.12.11) script, which also utilizes MATLAB scripts (R2023a; MathWorks), was used to automatically calculate distances and points within the spinal column using manually drawn MedCAD objects (MedCAD Custom Surgical Solutions; Figure 1). MedCAD objects are the 3D analytical objects within the DICOM coordinate system used for analysis in MIMICS, which can then be used to measure distances. These measurements included the following:

- The spinal cord width, height, and circumference;
- The spinal canal width and height;
- The left and right separation of the spinal cord and the canal; and
- The ventral and dorsal separation of the spinal cord and the canal.

The second group of measurements included an assessment of the disk height index (DHI), vertebral height, and neural foramina circumference. The DHI was calculated using a method described by Masuda and colleagues[16] Here, the MPR function was used with the 3D T1 transverse and where appropriate T2 TSE sagittal images to calculate the spacing between the endplates for the vertebrae cranial and caudal to each respective disk. These measurements were done at the ventral edge, midpoint, and dorsal edge for each cranial vertebra (measurements A, B, and C, respectively), caudal vertebrae (measurements G, H, I, respectively), and disk (measurements D, E, and F). The DHI was then calculated using Equation 1, with an example shown in Figure 2.

$$DHI = 2\frac{D+E+F}{A+B+C+G+H+I} \qquad \text{Equation 1}$$

Since vertebral height is inherent to the DHI calculation, CT was used instead of MR for maximal accuracy for the dorsal vertebral height measurements, corresponding to measurements A and G, reported separately in this work. Finally, the circumference, major and minor axis of the best-fit plane, and centroid of each neural foramina were calculated bilaterally by using 3D STL models generated from the CT acquisition (Figure 3). After acquisition and calculation of the parameters,

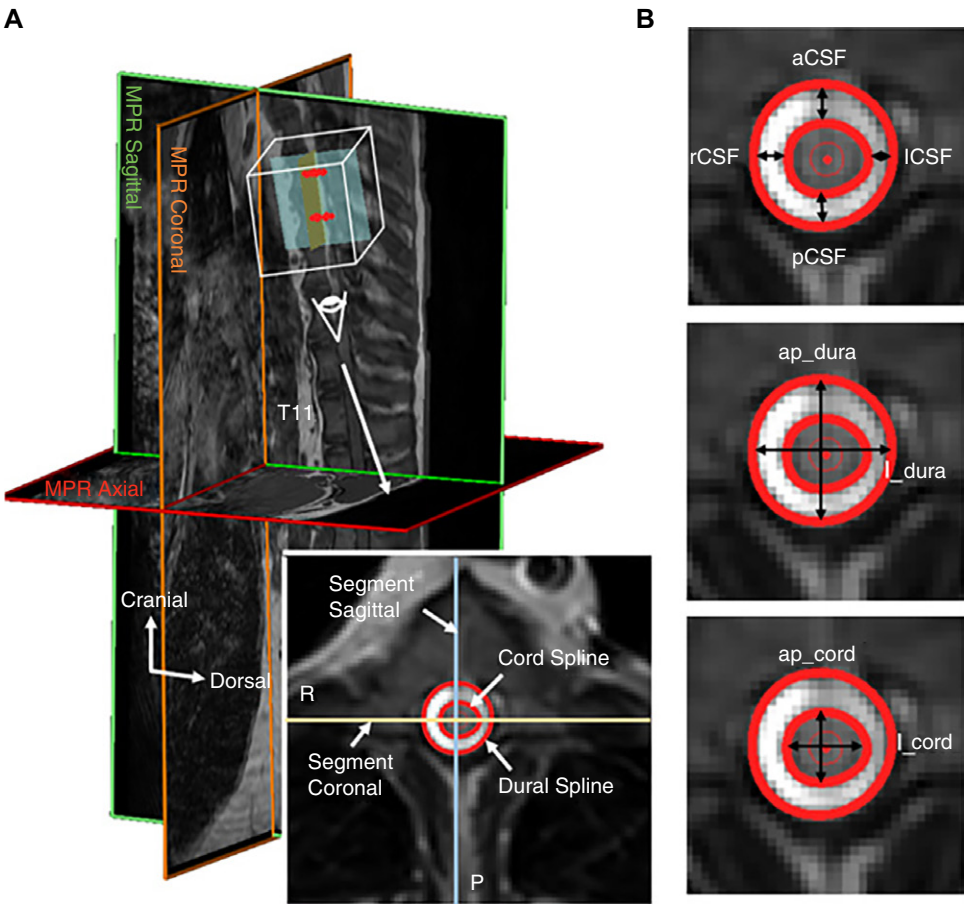

Figure 1. Representative segment from sheep 5 with planes and splines drawn. (A) Segment coronal (yellow) and sagittal (blue) planes, plus cord and dural splines, applied to a transverse slice at T7. (B) Derived dimensions: ventral and dorsal CSF thickness (aCSF and pCSF), left and right CSF thickness (lCSF and rCSF), edge-to-edge ventral-dorsal dural width (ap_dura), lateral dural height (l_dura), and ventral-dorsal cord height (ap_cord) and lateral cord width (l_cord).

review of the automated measurements confirmed integrity of automatic objects generated.

Results

All raw CT and MRI-derived data are available as supplementary Microsoft Excel files (Supplementary 1.MRI.data; Supplementary 2.CT.data). CT and MR images were successfully acquired in all animals; the CT images of 1 sheep were omitted because that sheep underwent CT with a different system (O-arm; Medtronic), and the resulting images were incompatible for analysis with the rest of the group, due to the reduced image details and reduced field of view inherent to O-arm imaging. Each sheep had 7 cervical and 13 thoracic vertebrae. Five of the sheep had 7 lumbar vertebrae but one had 6. Another sheep's C1 and C2 measurements were not available due to image edge distortion during processing. The conus medullaris was located between mid-L2 and upper-L5 for all animals. The calculated morphometrics for the first group of measurements are presented in Figure 4. Figure 4A illustrates the spinal cord circumference, which contains peaks at C6 (27.41 mm) and L6 (24.93 mm). Similarly, coronal spinal canal and cord (Figure 4C and D), which are indexes of height, have similar peaks at the same vertebrae. Lumbar sagittal spinal canal measurements, equivalent to width, had mean values ranging from 9.39 mm in L1, up to a consistent peak at L6 for all animals at 11.92 mm. Ventral-dorsal spine displacement, provided in 4G, although generally near the zero mark for all vertebrae, shows an average ventral displacement peak of 2.65 mm at L7. Displacement in the lateral dimension, aside from L7, shows a small, group-level right displacement of all vertebrae, up to 0.65 mm at C2. The DHIs, vertebral heights, and neural foramina circumferences, as derived using Equation 1 with the method shown in Figure 2, are provided for all animals in Figure 5. Left and right for aminal circumference, in Figure 5A and B, showed bimodal peaks at C7 and L7, a trough at T10, and a steep drop in circumference at the axis and atlas (C1/C2). DHI generally ranged from 0.11 to 0.22, with the larger values in the midthoracic levels. Finally, vertebral height showed a steady decline from L7 to T9, with a peak at C4 (40.42 mm), and a steep drop down to C1, similar to for aminal circumference.

Discussion

This study contributes to ovine modeling of neuromodulation and spinal treatments in several ways. Our methodology appears to give reasonable measurements for the model in line with previous literature, adds normative values for anatomy not previously examined, and allows for comparison to human measurements when planning experiments. This allows for the measurement of parameters with comparison to normative data before implantation of devices in an ovine model. It may also guide neuromodulation parameter configuration used in such models. Although the lumbosacral spine of the sheep has been measured via advanced MR imaging,[1,14] we are unaware of any studies that have quantified spine morphology of the cervical and thoracic vertebrae using advanced MR and CT imaging. In addition, several parameters such as dorsal CSF,

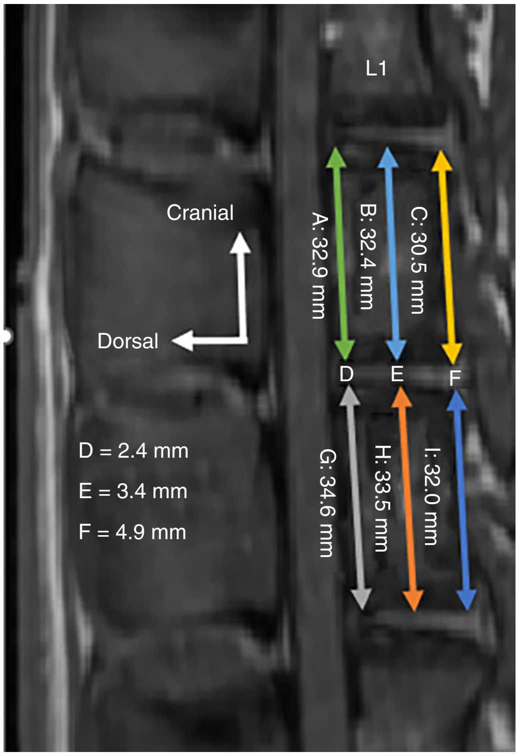

Figure 2. Representative disk height index (DHI) measurements at sagittal L2-L3 in ovine 1. Either the MPR 3D T1 transverse or T2 TSE sagittal images were used to calculate the spacing between the endplates for the vertebrae cranial and caudal to each respective disk. These measurements were done at the ventral edge, midpoint, and dorsal edge for each cranial vertebra (measurements A, B, and C, respectively), caudal vertebrae (measurements G, H, and I, respectively), and disk (measurements D, E, and F). In this example, the DHI is calculated at 0.11, based on the calculation from Equation 1.

spine displacement, and foramen circumference have been lacking in literature until now.

In the present study, we characterized the ovine cervical, thoracic, and lumbar spinal cord, dural canal, and CSF in 6 subjects. Compared with Mageed and colleagues,[1] who imaged 5 Merino sheep under CT and found a range of 9.8 to 18.9 mm for L1-L6, lumbar spinal canal width segments beyond L1 had a smaller width in our study. A study by Wilkes and colleagues[17] also dissected Merino sheep for anatomic measurement and found similarly larger width values, ranging from 11.5 to 17.5 mm for L1-L7. Our coronal spinal canal measurements, a length measurement, had a similar mean range. Therefore, compared with the older study by Wilkes and colleagues,[17] which also collected cervical and thoracic measurements, there was a similar pattern of our sagittal spinal canal segments being smaller, with coronal canal segments being of a comparable range. It is likely that there is variation between breeds, as we used a smaller, mixed breed of sheep for our study.[18] In addition, our utilization of a different imaging modality and processing procedure from previous studies[1,14] may yield variation. While Wilke and colleagues[17] provided some initial data on lumbar spine measurements, the data presented here is the first to provide similar measurements in the thoracic and cervical spine.

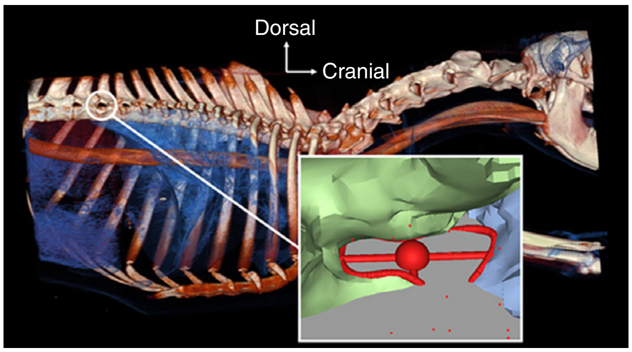

Figure 3. Representative neural foramen measurements in sheep 2. Using the CT images, the circumference, major axis (rostral-caudal line), minor axis (ventral-dorsal line), and centroid for each foramina (shown in the inset) were assessed in MIMICS. The image of the sheep in this figure was generated using the Volume Rendering Technique on the syngo.via workstation (Siemens Medical Solutions).

Our CT-derived measurements included foraminal circumference, vertebral height, and DHI. Compared with a study by Bai and colleagues[19] that compared anatomic human lumbar spine measurements to sheep and deer, our ovine vertebral heights were comparable, ranging from 31.78 to 35.60 mm. The similarity in lumbar spine measurements obtained from physical specimens supports the validity of our imaging procedure. Another study[20] compared cadaveric human L4 vertebrae to various animal models, including sheep. Vertebral body height for L4 in sheep was approximately 13% larger than humans in that study, at approximately 30 mm. Our measured body height was slightly larger at that vertebra, at approximately 35 mm (Figure 5D). Lumbar DHI was also comparable to previous studies in sheep, ranging from 15 to 20 units. Particularly, this is similar to a study by Reitmaier and colleagues[21] that investigated, using in vivo and in vitro ovine models, vertebral indexes following spine segment destabilization and fusion procedures. Overall, our ovine model measurements were validated by the existing lumbosacral measurements in the literature referenced above,[19–21] while providing new measurements and parameters including the cervical and thoracic spine.

While sharing many similarities, differences between ovine and human spine morphology should also be noted when planning experiments to model neuromodulation treatments so that necessary adjustments may be made. By measuring thoracic levels, normative data exist for anatomy relevant to spinal cord stimulation. A recent study evaluated thoracic morphometric measurements using preoperative MRI in 101 chronic pain patients who were to be implanted with SCS.[22] Human measurements of dorsal CSF thickness and spinal cord and canal variables were up to 2 times larger compared with the ovine measurements in our study. Specifically, thoracic dorsal CSF thickness was almost 2 times larger in humans, ranging from 3.9 to 4.1 mm. This may affect stimulation parameters and response to therapy amplitude in ovine models.[23] This difference in CSF distance between the spinal cord and epidural space where SCS leads are located manifests as comparatively larger spinal ECAP amplitudes in the sheep compared with humans, as more of the ECAP is shunted and lost in the greater CSF thickness in humans.[24] This may be further complicated by method selection when it comes to ECAP estimation, where sensitivity parameters are crucial for increasing signal-to-noise ratio for optimal and accurate application.[25] Overall, the value of ovine spine measurements comes from the similarity to human morphometry and the ability to account for the differences. For example, smaller dorsal CSF thickness may require lower stimulation amplitudes and affect coverage over ovine spinal cords. In addition, larger vertebral heights may require wider spacing of contacts during stimulation modeling of the effects of SCS, since the therapy targets the spinal cord anatomy itself, and not the vertebral bodies used as proxies during surgical

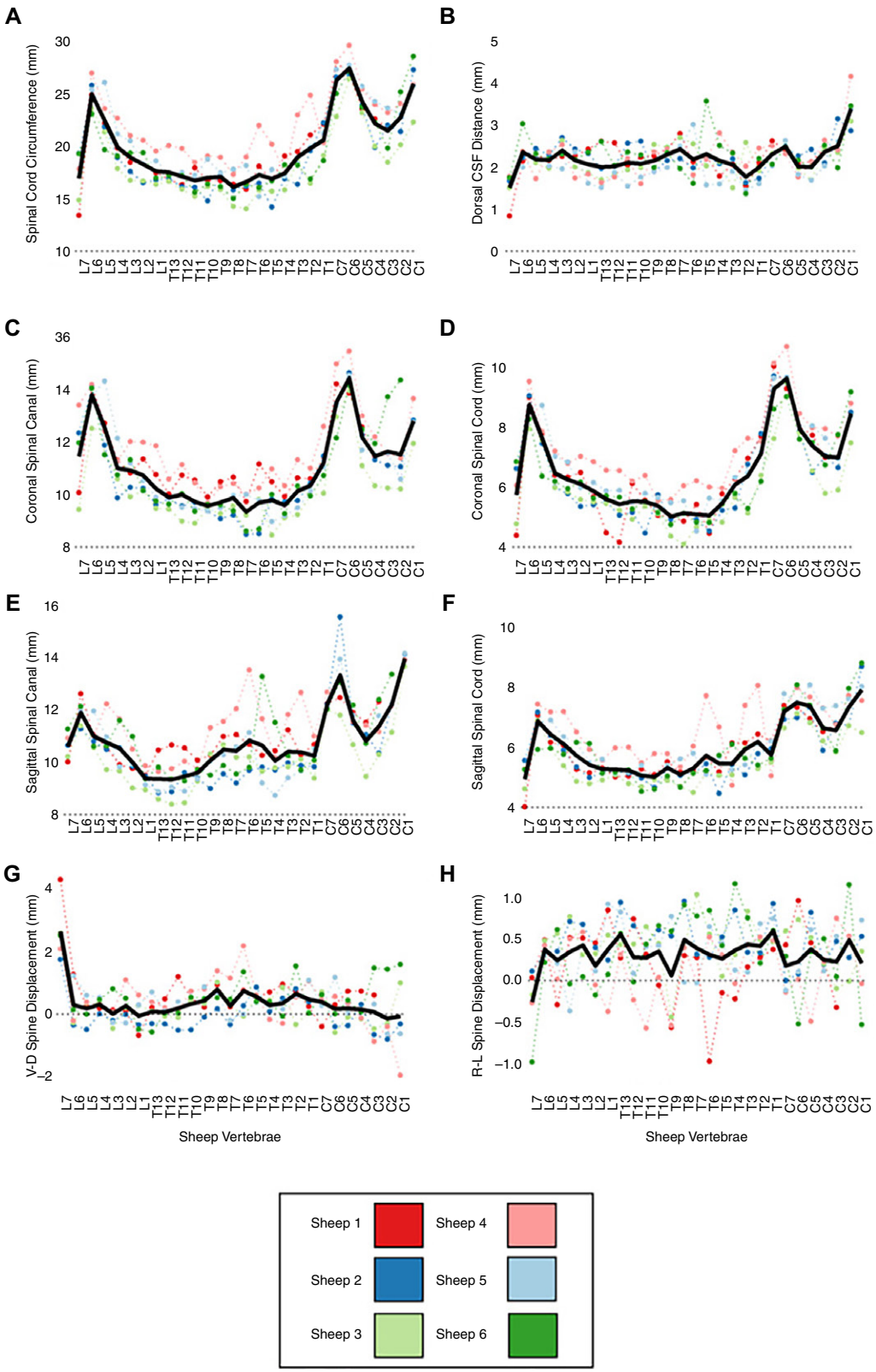

Figure 4. MRI T2 TSE-derived sheep spine morphometrics. Using the MPR function, several parameters were computed from sheep T2 MR imaging. (A–H) Images are ascending from lumbar to cervical vertebrae from left to right, with individual colors representing individual ovine and the mean in solid black line. The parameters include (A) spinal cord circumference; (B) dorsal CSF distance (equal to the dorsal distance); (C) coronal spinal canal; (D) spinal cord (both are height measurements); (E) sagittal spinal canal; (F) spinal cord (both are width measurements); (G) ventral-dorsal (V-D) spine displacement (ventral minus dorsal distance); and (H) right-left (R-L) spine displacement (right minus left distance).

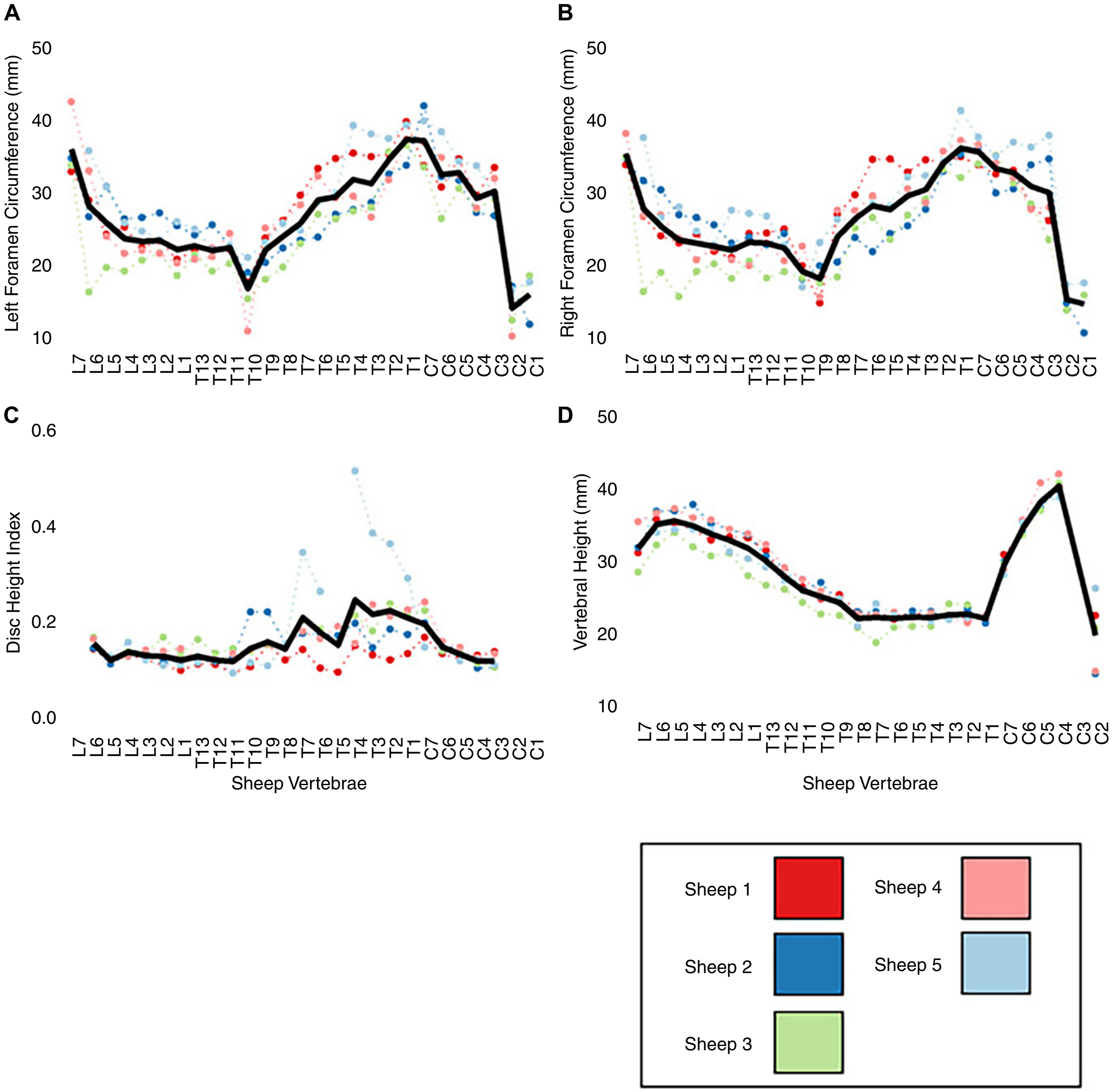

Figure 5. CT-derived ovine spine measurements and indices. Using STL models derived from the CT acquisitions, (A and B) left and right foramen circumference and (D) vertebral height were computed for every vertebra for each animal. (A–C) Images are ascending from lumbar to cervical vertebrae from left to right, with individual colors representing individual ovine and the mean in solid black line. Using the MPR function as well as Equation 1, the (C) disk height index was computed for each vertebra. All animals, except ovine 6, had a CT scan for use in CT measurements.

implantation. Another study[26] demonstrated a human neural foraminal circumference ranging from 47 to 55 mm. This is larger than the lower lumbar neural foramen measured in Figure 5 (ranging from 15.53 to 42.38 mm). Therefore, when using sheep as models for pain therapies occupying the foramen such as dorsal root ganglion stimulation,[27] it should be noted that implant size may need to be adjusted for the smaller corridor. As seen in these examples, this study provides comprehensive data useful in planning the exploration of stimulation-related therapies in an ovine model.

Using MR and CT imaging, this study produced measurements for the development of precision ovine models for the study of neurosurgical treatments. To our knowledge, this is the first study to quantify spine foraminal circumference for the entire ovine spine including the cervical and thoracic regions, which is a crucial measurement for modeling stimulation of dorsal root ganglion. In addition, our measurement of cervical and thoracic ovine spine provides novel data for the future development of ovine SCS using percutaneous or paddle leads in those regions, including cervical SCS, which has been shown to be effective in the management of chronic pain.[28] The study of spinal ECAPs provides critical information as they have been shown to be associated with perceived sensation in chronic pain patients and are affected by the posture of patients.[24,29] In addition, ECAPs in ovine models have been recently investigated and may become a powerful tool for the development of closed-loop SCS.[4,30] New data from the EVOKE clinical trial, which compared ECAP-controlled

closed-loop and open-loop paresthesia-centric SCS for the treatment of chronic pain, reported higher rates of leg and back pain reduction in patients receiving closed-loop tonic SCS.[31] The information presented in this work may be useful for investigating pain, somatosensation, and motor signals, as well as for accurate lesioning for disease models such as SCI and neuropathy.

The present study has limitations. Our sample size of 6 female subjects may not be generalizable to males or other breeds of sheep. However, we used a standardized protocol for imaging, and our measures were similar to previously published studies that investigated morphometry using imaging and cadaveric specimens. In addition, the animals were of various breeds, sizes, and age. Although we did not control for these parameters, the purpose of our study was to provide this quantitative data for future researchers to use for their investigations. Furthermore, the variations in age and size are similar to other previously discussed studies.[1,4,5,7,9-11]Another limitation is the fact that the sheep used in this study did not employ a chronic pain model. While we do not necessarily expect this to affect the anatomy of the sheep, they may experience less degenerative changes to parameters limiting generalizability to clinical populations with chronic pain (e.g., use of SCS for chronic low-back pain).

Conclusion Using MR and CT imaging, the entire ovine spine anatomy, including cord and foraminal circumference, vertebral displacement and height, and dorsal CSF space across all spine segments was quantified in a study population. This enhances the utilization of ovine models in the study of spinal treatments such as closed-loop SCS, novel interventional pain therapies, and the study of veterinary neurologic disease.

Supplementary Materials

Supplementary Data 1 – MRI-derived measurements of ovine spine. These individualized measurements include right, left, anterior, and posterior distances; coronal spinal cord and canal; sagittal spinal cord and canal; spinal cord and CSF circumference SC (all in mm); radiographic midline in degrees, level of conus medullaris , and total cord length. Individualized data for each subject provided as separate excel sheets. Final sheet ("Pics") provides visualization of how measures were obtained using MedCAD objects.

Supplementary Data 2 – CT-derived measurements of ovine spine. These individualized measurements include disc height index (DHI) measurements as described in Equation 1 and Figure 2; calculated DHI; left and right foraminal MRI and CT-derived spine length (in mm); spinal canal length (in mm); and posterior canal height (in mm). Individualized data for each subject provided as separate excel sheets for the five subjects which were imaged using CT. The "Template" and "Foramen-Canal CT Script" were used to generate the measures and populate the individual sheets.

Conflict of Interest

N.M.B., T.B., and D.D. are employees of Medtronic plc. Y.S.O and K.H. have no disclosures.

No AI-assisted technologies were used in the generation of this manuscript.

Funding

This study was funded by Medtronic plc.

Author Contributions

Y.S.O. – data visualization, manuscript drafting, review, and editing; N.M.B. – imaging and data analysis, manuscript drafting, data visualization, review, and editing; T.B. – animal care coordination, data collection, imaging protocol preparation, review, and editing; D.D. – study design, study supervision, manuscript drafting, review, and editing; K.H. – study supervision, review, and editing.

Data Availability

The raw data used in this work can be made available upon request at the discretion of the authors. Requests to access the datasets should be directed to David Dinsmoor at david.a.dinsmoor@medtronic.com.

References

1. Mageed M, Berner D, Jülke H, Hohaus C, Brehm W, Gerlach K. Morphometrical dimensions of the ovine thoracolumbar vertebrae as seen on digitised CT images. *Lab Anim Res.* 2013;29(3):138–147.
2. Jensen MP, Brownstone RM. Mechanisms of spinal cord stimulation for the treatment of pain: still in the dark after 50 years. *Eur J Pain.* 2019; 23(4):652–659.
3. Caylor J, Reddy R, Yin S, et al. Spinal cord stimulation in chronic pain: evidence and theory for mechanisms of action. *Bioelectron Med.* 2019;5:1–41.
4. Dinsmoor DA, Usoro JO, Barka ND, Billstrom TM, Litvak LM, Poree LR. Using evoked compound action potentials to quantify differential neural activation with burst and conventional, 40 Hz spinal cord stimulation in ovines. *Pain Rep.* 2022;7(6):e1047.
5. Gibson-Corley KN, Oya H, Flouty O, et al. Ovine tests of a novel spinal cord neuromodulator and dentate ligament fixation method. *J Invest Surg.* 2012;25(6):366–374.
6. Safayi S, Jeffery ND, Fredericks DC, et al. Biomechanical performance of an ovine model of intradural spinal cord stimulation. *J Med Eng Technol.* 2014;38(5):269–273.
7. Reddy CG, Miller JW, Abode-Iyamah KO, et al. Ovine model of neuropathic pain for assessing mechanisms of spinal cord stimulation therapy via dorsal horn recordings, von Frey filaments, and gait analysis. *J Pain Res.* 2018; 11:1147–1162.
8. Flouty OE, Oya H, Kawasaki H, et al. Intracranial somatosensory responses with direct spinal cord stimulation in anesthetized ovine. *PLoS One.* 2013;8(2):e56266.
9. Wilson S, Abode-Iyamah KO, Miller JW, et al. An ovine model of spinal cord injury. *J Spinal Cord Med.* 2017;40(3):346–360.
10. Wilson S, Fredericks DC, Safayi S, et al. Ovine hemisection model of spinal cord injury. *J Invest Surg.* 2021;34(4):380–392.
11. Wallace AN, Hillen TJ, Friedman MV, et al. Percutaneous spinal ablation in a sheep model: protective capacity of an intact cortex, correlation of ablation parameters with ablation zone size, and correlation of postablation MRI and pathologic findings. *AJNR Am J Neuroradiol.* 2017;38(8):1653–1659.
12. Li Z, Zhai S, Liu S, et al. A sheep model of chronic cervical compressive myelopathy via an implantable wireless compression device. *Eur Spine J.* 2022;31(5):1219–1227.
13. Toossi A, Bergin B, Marefatallah M, et al. Comparative neuroanatomy of the lumbosacral spinal cord of the rat, cat, pig, monkey, and human. *Sci Rep.* 2021;11(1):1955.
14. Bouhsina N, Decante C, Hardel JB, et al. Comparison of MRI T1, T2, and T2* mapping with histology for assessment of intervertebral disc degeneration in an ovine model. *Sci Rep.* 2022;12(1):5398.
15. Nisolle JF, Bihin B, Kirschvink N, et al. Prevalence of age-related changes in ovine lumbar intervertebral discs during computed tomography and magnetic resonance imaging. *Comp Med.* 2016;66(4):300–307.
16. Masuda K, Aota Y, Muehleman C, et al. A novel rabbit model of mild, reproducible disc degeneration by an anulus needle puncture: correlation between the degree of disc injury and radiological and histological appearances of disc degeneration. *Spine (Phila Pa 1976).* 2005;30(1):5–14.
17. Wilke HJ, Kettler A, Wenger KH, Claes LE. Anatomy of the ovine spine and its comparison to the human spine. *Anat. Rec.* 1997;247(4):542–555.
18. Posbergh CJ, Huson HJ. All ovines and sizes: a genetic investigation of mature body size across ovine breeds reveals a polygenic nature. *Anim Genet.* 2021;52(1):99–107.
19. Bai X, Liu G, Xu C, et al. Morphometry research of deer, ovine, and human lumbar spine: feasibility of using deer and ovine in spinal animal models. *Int J Morphol.* 2012;30(2):510–520.

20. McLain RF, Yerby SA, Moseley TA. Comparative morphometry of L4 vertebrae: comparison of large animal models for the human lumbar spine. *Spine (Phila Pa 1976).* 2002;27(8):E200–E206.
21. Reitmaier S, Schuelke J, Schmidt H, Volkheimer D, Ignatius A, Wilke HJ. Spinal fusion without instrumentation–experimental animal study. *Clin Biomech (Bristol).* 2017;46:6–14.
22. Hines K, Tran C, Koka A, et al. Thoracic canal morphology on preoperative magnetic resonance imaging in spinal cord stimulation patients. *Pain Pract.* 2024;24(8):1035–1041.
23. Gmel GE, Santos Escapa R, Parker JL, Mugan D, Al-Kaisy A, Palmisani S. The effect of spinal cord stimulation frequency on the neural response and perceived sensation in patients with chronic pain. *Front Neurosci.* 2021;15:625835.
24. Brucker-Hahn MK, Zander HJ, Will AJ, et al. Evoked compound action potentials during spinal cord stimulation: effects of posture and pulse width on signal features and neural activation within the spinal cord. *J Neural Eng.* 2023;20(4):046028.
25. Chakravarthy K, FitzGerald J, Will A, et al. A clinical feasibility study of spinal evoked compound action potential estimation methods. *Neuromodulation.* 2022;25(1):75–84.
26. Nowak P, Dąbrowski M, Druszcz A, Kubaszewski Ł. The spatial characteristics of intervertebral foramina within the L4/L5 and L5/S1 motor segments of the spine. *Appl. Sci.* 2024;14(6):2263.
27. Deer TR, Levy RM, Kramer J, et al. Dorsal root ganglion stimulation yielded higher treatment success rate for complex regional pain syndrome and causalgia at 3 and 12 months: a randomized comparative trial. *Pain.* 2017;158(4):669–681.
28. Deer TR, Skaribas IM, Haider N, et al. Effectiveness of cervical spinal cord stimulation for the management of chronic pain. *Neuromodulation.* 2014;17(3):265–271.
29. Chakravarthy K, Bink H, Dinsmoor D. Sensing evoked compound action potentials from the spinal cord: novel preclinical and clinical considerations for the pain management researcher and clinician. *J Pain Res.* 2020;13:3269–3279.
30. He J, Barolat G, Holsheimer J, Struijk JJ. Perception threshold and electrode position for spinal cord stimulation. *Pain.* 1994;59(1):55–63.
31. Mekhail NA, Levy RM, Deer TR, et al. ECAP-controlled closed-loop versus open-loop SCS for the treatment of chronic pain: 36-month results of the EVOKE blinded randomized clinical trial. *Reg Anesth Pain Med.* 2024;49(5):346–354.